Proceedings of the 2004 IEEE International Conference on Control Applications, pp. 131-136, September 2-4, Taipei, Taiwan, 2004

Jin-Hua She, Yasuhiro Ohyama,
Hiroyuki Kobayashi
School of Bionics, Tokyo Univ. of Tech.
1404-1 Katakura, Hachioji
Tokyo, 192-0982, Japan
{she, ohyama, yagshi}@bs.teu.ac.jp

Tetsuya Suzuki
Sigmatron Co., Ltd.
3-3-5 Kudannkita, Chiyoda-Ku,
Tokyo, 102-0073 Japan
tetsuagu@bitcat.net

***Abstract*— A three-wheeled electric cart was developed for the elderly and people undergoing rehabilitation. A bilateral master-slave system configuration is employed to control the speed of the cart, and the controller was designed based on H_∞ control theory. The main feature of the system is that the load added to the pedals can easily be adjusted with a speed-adjustment program to suit the strength of the driver. Experimental results on a fabricated cart demonstrate the validity and effectiveness of the design methodology.**

I. INTRODUCTION

Japan is rapidly becoming an aging society. According to an annual report on aging from the Cabinet Office of the Government of Japan [1], the percentage of old people (over 65 years old) in the population was 18.5% in 2002. This percentage will continue to increase, reaching 26.0% in 2015 and 35.7% in 2050. Since this is becoming a very serious social problem, policies to deal with an aging society and their implementation have received considerable attention; and the health and welfare of the elderly has become one of the main concerns of the government. In response to this concern, a great deal of research and development related to the health care of old people has been carried out over the last few years. To improve the ability of old people to get around, many companies have developed electric carts, which have recently begun to appear on the market. However, since almost all of the commercially available carts were designed solely as a means of transportation, no consideration was given to an elderly person's need for physical exercise, Thus, a reliance on these carts for getting around can ultimately result in the deterioration of the user's leg and back muscles.

The purpose of this study was to develop a three-wheeled electric cart that not only is a means of transportation, but also provides the driver with a way of getting some physical exercise. The cart has two foot pedals, and the load added to the pedals can be adjusted with a speed-adjustment program to suit the physical condition of the driver. A bilateral master-slave system configuration is employed to control the speed of the cart; and H_∞ control theory was used to design the controller.

II. SYSTEM CONFIGURATION AND DESIGN

The electric cart developed in this study is shown in Fig. 1. It is based on the Everyday Type-S, a commercially-available ready-made three-wheeled cart (Araco Corp., Japan). As a way of providing physical exercise, two pedals were mounted on it. The system employs an electrical rather than a mechanical connection between the pedals and the drive wheels; and a motor connected to the pedals generates the load, which is the amount of additional resistance that the driver feels when the pedals are pushed. These modifications enable the driver to easily adjust the load to suit his or her physical condition. The load added to the pedals is also responsive to the road conditions so as to provide a more realistic driving experience.

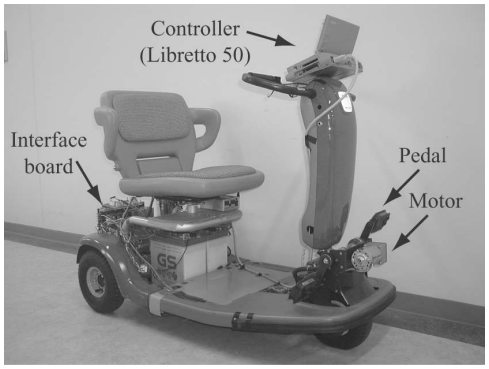

Fig. 1. Photograph of electric cart.

A. System Configuration

The controlled output of the cart system includes position, speed and/or force. Since a first-order plant is easy for humans to operate in a cooperative human-machine system [5], speed was selected as the controlled output. The system employs a master-slave configuration (e.g., [2]) and two motors. When the driver pushes the pedals with a torque $\tau(t)$, the pedal motor (master) turns with a rotational speed $v_m(t)$. This is used as a reference speed for the cart motor (slave), which drives the cart. The speed at which the cart moves is proportional to the rotational speed, $v_s(t)$, of the cart motor. The error between $v_m(t)$ and $v_s(t)$ is fed back to the controller of the cart motor to generate a control input for it so that the speed of the cart motor can track the speed of the pedal motor. In addition, to enable the driver to perform an appropriate level of physical exercise, the pedal motor can be set to make the pedals more difficult or easier to turn. And a bilateral scheme (e.g., [3], [4]) is used that also feeds the error between $v_m(t)$ and $v_s(t)$ back to the pedal motor,

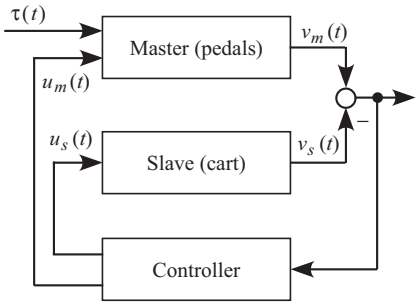

Fig. 2. Configuration of bilateral master-slave cart system.

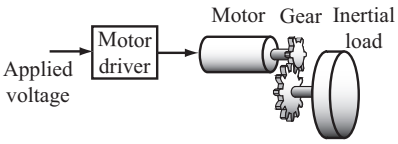

Fig. 3. Structure of master-slave system.

so that the driver can feel the road conditions and obtain a more realistic driving experience. The configuration of the bilateral master-slave cart system is shown in Fig. 2.

In the designed system, the speed at which the pedals turn the pedal motor is determined by the driver's efforts, and constitutes a reference input for the cart. The designed controller makes the speed of the cart motor track that reference. So, the experience is very similar to riding a bicycle.

B. Modelling

The pedal and cart system is the same as that shown in Fig. 3.

The master (the pedals) is described by the following equation.

$$\begin{cases} \dfrac{dv_m(t)}{dt} = A_m v_m(t) + B_m u_m(t) + B_\tau \tau(t), \\ A_m = \dfrac{c_m}{J_m},\ B_m = \dfrac{k_m}{J_m},\ B_\tau = \dfrac{1}{J_m}. \end{cases} \tag{1}$$

Since it is difficult to determine B_τ precisely, a new variable, $\tau'(t) := B_\tau \tau(t)$, was introduced, which allows the mathematical model of the master to be rewritten as ($B'_\tau = 1$)

$$\frac{dv_m(t)}{dt} = A_m v_m(t) + B_m u_m(t) + B'_\tau \tau'(t). \tag{2}$$

The dynamics of the slave (the cart) depends on the weight of the driver. Assuming the weight of the driver to be between 45 kg and 100 kg yields

$$\begin{cases} \dfrac{dv_s(t)}{dt} = A_s(t) v_s(t) + B_s(t) u_s(t), \\ A_s(t) = \dfrac{c_s}{J_s(t)} := A_{s0} + \Phi \Gamma(t) \Psi_A, \\ B_s(t) = \dfrac{k_s}{J_s(t)} := B_{s0} + \Phi \Gamma(t) \Psi_B, \\ \Gamma^2(t) \le 1. \end{cases} \tag{3}$$

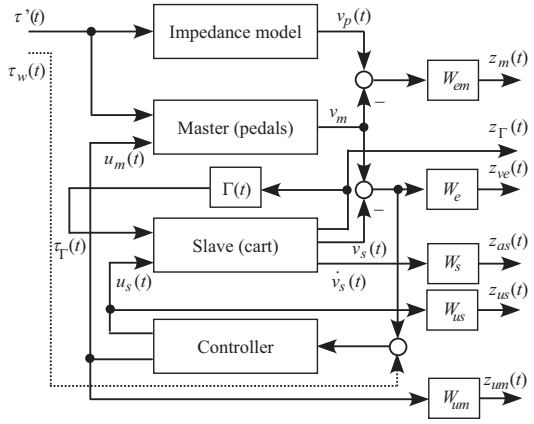

Fig. 4. Block diagram used for design of H_∞ controller.

In (1), (2) and (3), $u_m(t)$ and $u_s(t)$ are the voltages applied to the pedal and cart motors, J_m ($J_s(t)$) is the moment of inertia of the master (slave) motor, c_m (c_s) is the frictional damping constant of the master (slave), and k_m (k_s) is the voltage gain of the master (slave) motor driver. The experimentally obtained values of the parameters are:

$$\begin{cases} A_m = -1.49, & B_m = 2.45, \\ A_{s0} = -0.24, & B_{s0} = 2.08, \\ \Phi = [1\ 1], & \\ \Psi_A = [0.04\ \ 0]^T, & \Psi_B = [0\ \ 0.69]^T. \end{cases} \tag{4}$$

C. Formulation of Control Problem

Instead of the load on the pedals being transmitted mechanically by means of a chain, in this study the pedal and cart motors were connected electrically, and an impedance model was used to describe the feeling of pushing the pedals. The model is given by

$$\frac{dv_p(t)}{dt} = A_p v_p(t) + B_p \tau'(t), \tag{5}$$

where A_p and B_p are constants. The feeling depends on the values of A_p and B_p. The system contains three impedance models for three different modes of operation:

$$\begin{cases} A_p = -1.49, & B_p = 2.00 \quad (\text{Model A}: \text{ Strenuous Mode}); \\ A_p = -1.49, & B_p = 3.49 \quad (\text{Model B}: \text{ Neutral Mode}); \\ A_p = -1.49, & B_p = 3.90 \quad (\text{Model C}: \text{ Assisted Mode}). \end{cases} \tag{6}$$

We formulate the design problem for the controller using a common H_∞ control formulation. The exogenous input signal is $\tilde{\tau}(t) := [\tau'(t)\ \tau_\Gamma(t)]$, and the controlled outputs are: (a) the weighted speed error between the impedance model and the pedals, $z_m(t)$; (b) the input signal of the uncertainty $\Gamma(t)$, $z_\Gamma(t)$; (c) the weighted speed error between the pedals and the wheels, $z_{ve}(t)$; (d) the weighted acceleration of the cart, $z_{as}(t)$, in order to take riding comfort into account; and (e) the weighted voltages applied to the pedal and cart motors, $z_{us}(t)$ and $z_{um}(t)$, in order to keep them at a low

level. The block diagram used for the design of the cart control system is shown in Fig. 4. Now, the design problem for the controller can be stated as follows:

Find a controller $K(s)$ such that

1) *the cart control system is internally stable, and*
2) *the H_∞ norm of the transfer function from $\tilde{\tau}(t)$ to $z(t) := [z_m(t)\ z_\Gamma(t)\ z_{ve}(t)\ z_{as}(t)\ z_{us}(t)\ z_{um}(t)]^T$, $G_{z\tau}(s)$, is less than 1, i.e., $\|G_{z\tilde{\tau}}(s)\|_\infty < 1$.*

D. H_∞ Controller

The following weighting transfer functions are used [8], [9], [10] in the design of the H_∞ controller:

$$\begin{cases} W_{em}(s) = W_e(s) = \dfrac{0.01s+1}{100s+1} = \left[\begin{array}{c|c} A_e & B_e \\ \hline C_e & D_e \end{array}\right], \\ W_s(s) = \dfrac{0.48}{0.812s+1} = \left[\begin{array}{c|c} A_a & B_a \\ \hline C_a & 0 \end{array}\right], \\ W_{um}(s) = W_{us}(s) = \dfrac{s+0.1}{s+1} = \left[\begin{array}{c|c} A_u & B_u \\ \hline C_u & D_u \end{array}\right], \end{cases} \tag{7}$$

where $G(s) = D + C(sI - A)^{-1}B$ is abbreviated to $G(s) = \left[\begin{array}{c|c} A & B \\ \hline C & D \end{array}\right]$. The corresponding Bode plots are shown in Fig. 5. In order to suppress the tracking error between $v_p(t)$ and $v_m(t)$, and between $v_m(t)$ and $v_s(t)$ in the steady state, low-pass weighting functions were chosen for $W_{em}(s)$ and $W_e(s)$. To suppress the applied control voltages, $u_m(t)$ and $u_s(t)$, to the pedal and cart motors during the transient response, high-pass weighting functions were chosen for $W_{um}(s)$ and $W_{us}(s)$. Riding comfort is also a very important criterion in evaluating control. The limits on the vibrations to which an operator should be exposed are defined in [11]. Fig. **??** shows the limit for whole-body vibration in the fore-and-aft directions over a period of 25 min. A direct calculation yielded $W_{s(\mathrm{ISO})}(s) = 0.8/(0.812s+1)$. However,

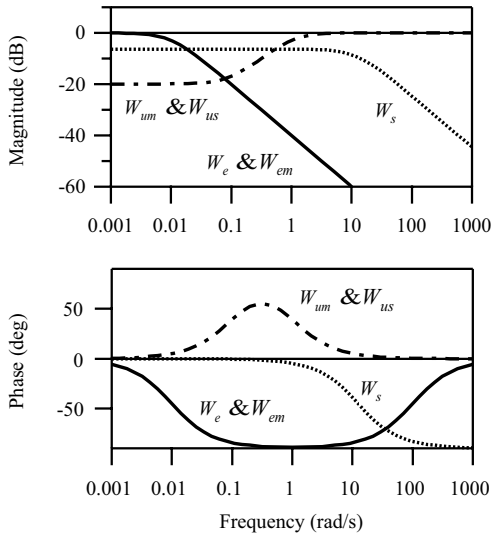

Fig. 5. Bode plots of weighting functions.

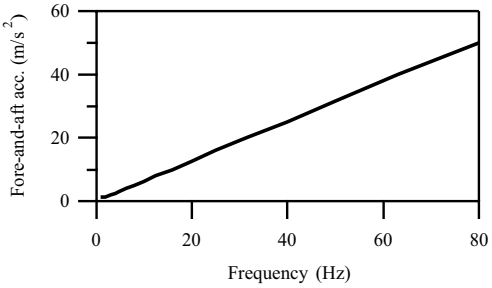

Fig. 6. Limit on whole-body vibrations in fore and aft directions to which operator is exposed over a period of 25 min [11].

since no H_∞ controller could be found for this function, we introduced a gain factor α to adjust the weighting function and let $W_s(s) = 0.8\alpha/(0.812s+1)$. Trial and error showed that there exists an H_∞ controller for a $\alpha = 0.6$. Thus, the $W_s(s)$ in (7) was selected. In order to relax the solvable condition and obtain a satisfactory H_∞ controller, a disturbance, $\tau_w(t)$, was added to the measurement output channel. Finally, the generalized plant is given by

$$\left[\begin{array}{c} \dot{x}(t) \\ \hline z(t) \\ y(t) \end{array}\right] = \left[\begin{array}{c|cc} A & B_1 & B_2 \\ \hline C_1 & D_{11} & D_{12} \\ C_2 & D_{21} & 0 \end{array}\right] \left[\begin{array}{c} x(t) \\ \hline w(t) \\ u(t) \end{array}\right], \tag{8}$$

where

$$\begin{aligned} y(t) &:= v_m(t) - v_s(t) + \tau_w(t), \\ w(t) &:= [\tau(t)\ \tau_\Gamma(t)\ \tau_w(t)]^T, \\ u(t) &:= [u_s(t)\ u_m(t)]^T, \end{aligned}$$

and

$$A = \begin{bmatrix} A_p & 0 & 0 & 0 & 0 & 0 & 0 & 0 \\ 0 & A_m & 0 & 0 & 0 & 0 & 0 & 0 \\ 0 & 0 & A_{s0} & 0 & 0 & 0 & 0 & 0 \\ B_e & -B_e & 0 & A_e & 0 & 0 & 0 & 0 \\ 0 & B_e & -B_e & 0 & A_e & 0 & 0 & 0 \\ 0 & 0 & B_a A_{s0} & 0 & 0 & A_a & 0 & 0 \\ 0 & 0 & 0 & 0 & 0 & 0 & A_u & 0 \\ 0 & 0 & 0 & 0 & 0 & 0 & 0 & A_u \end{bmatrix},$$

$$B_1^T = \begin{bmatrix} B_p^T & {B'_\tau}^T & 0 & 0 & 0 & 0 & 0 & 0 \\ 0 & 0 & \Phi^T & 0 & 0 & (B_a\Phi)^T & 0 & 0 \\ 0 & 0 & 0 & 0 & 0 & 0 & 0 & 0 \end{bmatrix},$$

$$B_2^T = \begin{bmatrix} 0 & 0 & B_{s0}^T & 0 & 0 & (B_a B_{s0})^T & B_u^T & 0 \\ 0 & B_m^T & 0 & 0 & 0 & 0 & 0 & B_u \end{bmatrix},$$

$$C_1 = \begin{bmatrix} D_e & -D_e & 0 & C_e & 0 & 0 & 0 & 0 \\ 0 & 0 & \Psi_A & 0 & 0 & 0 & 0 & 0 \\ 0 & D_e & -D_e & 0 & C_e & 0 & 0 & 0 \\ 0 & 0 & C_a A_{s0} & 0 & 0 & 0 & 0 & 0 \\ 0 & 0 & 0 & 0 & 0 & 0 & C_u & 0 \\ 0 & 0 & 0 & 0 & 0 & 0 & 0 & C_u \end{bmatrix},$$

$$C_2 = \begin{bmatrix} 0 & 1 & -1 & 0 & 0 & 0 & 0 & 0 \end{bmatrix},$$

$$D_{11}^T = \begin{bmatrix} 0 & 0 & 0 & 0 & 0 & 0 \\ 0 & 0 & (C_a\Phi)^T & 0 & 0 & 0 \\ 0 & 0 & 0 & 0 & 0 & 0 \end{bmatrix},$$

$$D_{12}^T = \begin{bmatrix} \Phi_B^T & 0 & 0 & (C_a B_{s0})^T & D_u^T & 0 \\ 0 & 0 & 0 & 0 & 0 & D_u^T \end{bmatrix},$$
$$D_{21} = \begin{bmatrix} 0 & 0 & 1 \end{bmatrix}.$$

Clearly, (A, B_2) is stabilizable and (C_2, A) is detectable. An H_∞ controller guaranteeing that $\|G_{zw}(s)\|_\infty < 1$ ($G_{zw}(s)$ is the transfer function from $w(t)$ to $z(t)$) exists if and only if $\mathcal{L}_D \neq 0$ [6] where

$$\mathcal{L}_D := \Big\{ (X, Y) \in \Re^{9\times 9} \times \Re^{9\times 9} : X > 0, Y > 0, L_B(X) < 0, L_C(Y) < 0, \begin{bmatrix} X & I \\ I & Y \end{bmatrix} \geq 0 \Big\},$$
$$L_B(X) = \begin{bmatrix} B_2 \\ D_{12} \end{bmatrix}^{\perp} Q_X \begin{bmatrix} B_2 \\ D_{12} \end{bmatrix}^{\perp T},$$
$$L_C(Y) = \begin{bmatrix} C_2^T \\ D_{21}^T \end{bmatrix}^{\perp} Q_Y \begin{bmatrix} C_2^T \\ D_{21}^T \end{bmatrix}^{\perp T},$$
$$Q_X = \begin{bmatrix} AX + XA^T + B_1 B_1^T & XC_1^T + B_1 D_{11}^T \\ C_1 X + D_{11} B_1^T & D_{11} D_{11}^T - I \end{bmatrix},$$
$$Q_Y = \begin{bmatrix} YA + A^T Y + C_1^T C_1 & YB_1 + C_1^T D_{11} \\ B_1^T Y + D_{11}^T C_1 & D_{11}^T D_{11} - I \end{bmatrix}.$$

The H_∞ controller is easily obtained by using the LMI Toolbox [7].

III. EXPERIMENTS

The validity of the designed H_∞ controller was verified through experiments. A Libretto 50 notebook computer (CPU: 75-MHz Pentium; Memory: 16 MB; Toshiba), was used for the controller; and an interface board (Fig. 7) was assembled to handle the input and output signals for the master and slave. Each of the three impedance models (A, B, C) (6) was tested under three road conditions: flat road, 5° uphill slope, and 5° downhill slope.

Typical experimental results are shown in Figs. 8–10 for a driver who weighed 63 kg. Fig. 8 is for a flat road. In this case, during the steady state (the period $[15\ \text{s},\ 25\ \text{s}]$), the average input voltages to the cart, $\bar{u}_s$, produced by the H_∞ controller were -0.462 V, -0.047 V and 0.377 V for Models A, B and C, respectively. The negative value for Model A means that an extra load was produced for the driver. On the other hand, Model B produced virtually no load because $\bar{u}_s$ is almost zero. And the positive value for Model C means that the driver was assisted. The 2 Hz vibration in the speed of the pedals is due to the driver's pushing the pedals.

The results for the uphill slope are shown in Fig. 9. The average voltages during the steady state (the period $[15\ \text{s},\ 25\ \text{s}]$) were -0.993 V, -0.088 V and 0.866 V for Models A, B and C, respectively. Clearly, while the Neutral Mode (Model B) guaranteed that the voltage input to the cart remained at a very low level, Models A and C provided a larger extra load or more assistance to the driver than those for the flat road. This reflected the actual road conditions and gave the driver more of a feeling of really driving, thus providing more sensory stimulation.

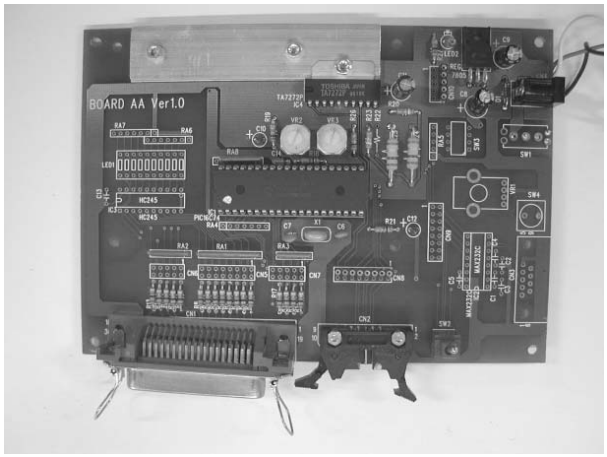

(a)

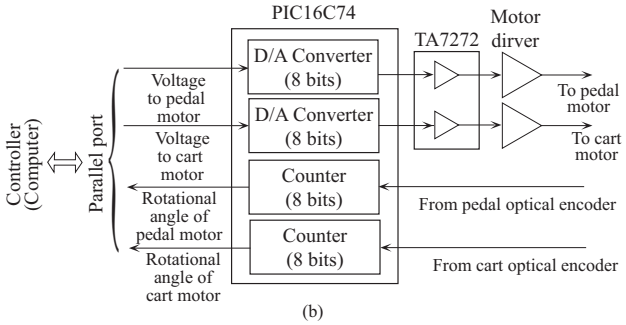

(b)

Fig. 7. Interface board: (a) Photo; (b) Block diagram.

The results for the downhill slope are shown in Fig. 10. The average voltages during the steady state (the period $[15\ \text{s},\ 25\ \text{s}]$) were -0.105 V, 0.003 V and 0.097 V for Models A, B and C, respectively. Note that, in this case, while the voltage input to the cart under the Neutral Mode (Model B) still remained at a very low level, Models A and C provided a smaller extra load or less assistance to the driver than those for the flat road. Thus, the system is responsive to the road conditions.

The average input voltages for the various conditions and models during the steady state (15–25 s) are listed in Table I.

IV. CONCLUSIONS

A three-wheeled electric cart has been developed for the elderly and people undergoing rehabilitation. The cart has two foot pedals, and the load added to the pedals can easily be

TABLE I

AVERAGE INPUT VOLTAGES DURING THE PERIOD 15 - 25 S.

	Extra-Load Mode	No-Load Mode	Assisted Mode
Flat	-0.462	-0.047	0.377
Uphill	-0.993	-0.088	0.866
Downhill	-0.105	0.003	0.097

adjusted with a speed-adjustment program to suit the physical condition of the driver. A bilateral master-slave system was built to control the speed of the cart. So, unlike most of the electric carts that are currently available, this one not only is a vehicle, but also provides the driver with some physical exercise. The controller was designed using H_∞ control theory. The validity of the designed H_∞ controller was tested under various load and road conditions. The experimental results show that this system configuration and the designed controller are useful for providing an appropriate level of physical exercise.

V. REFERENCES

[1] Cabinet Office, *Annual Report on the Aging Society 2001-2002 (in English), 2002-2003 (in Japanese)*, Available: `http://www8.cao.go.jp/kourei/`

[2] H. Kazerooni, T.-I. Tsay and K. Hollerbach, "A Controller Design Framework for Telerobotic Systems", *IEEE Trans. Contr. Syst. Technol.*, vol. 1, pp. 50-62, Mar. 1993.

[3] Y. Yokokohji and T. Yoshikawa, "Bilateral Control of Master-Slave Manipulators for Ideal Kinesthetic Coupling—Formulation and Experiment", *IEEE Trans. Robot. Automat.*, vol. 5, pp. 605-620, Oct. 1994.

[4] W.-H. Zhu and S. E. Salcudean, "Stability Guaranteed Teleoperation: An Adaptive Motion/Force Control Approach", *IEEE Trans. Automat. Contr.*, vol. 45, pp. 1951-1969, Nov. 2000.

[5] T. Inaba and Y. Matsuo, "Loop-shaping Characteristics of a Human Operator in a Force Reflective Manual Control System", *Proc. 1997 IEEE Int. Conf. on System, Man, and Cybernetics*, pp. 3621-3625, 1997.

[6] X. Xin, "Reduced-order controllers for the H_∞ control problem with unstable invariant zeros", *Automatica*, vol. 40, pp. 319-326, 2004.

[7] P. Gahinet, A. Nemirovski, A. J. Laub and M. Chilali, *LMI Control Toolbox*, The MathWorks, Natick, MA; 1995.

[8] M. G. Ortega and F. R. Rubio, "Systematic design of weighting matrices for the H_∞ mixed sensitivity problem", *J. Process Control*, vol. 14, pp. 89-98, 2004.

[9] T. Hiromatsu, T. Inaba and Y. Matsuo, "Development of an Electromechanical Active-Cab-Suspension", *Proc. IEEE Int. Conf. on Industrial Electronics, Control, and Instrumentation (IECON'93)* , pp. 2132-2137, 1993.

[10] J. Yan and S. E. Salcudean, "Teleoperation Controller Design Using H_∞ Optimization with Application to Motion-Scaling", *IEEE Trans. Contr. Syst. Technol.*, vol. 4, pp. 244-258, May 1996.

[11] ISO, *ISO Standards Handbook: Mechanical vibration and shock*, vol. 2, Ed. 2, ISO, 1995.

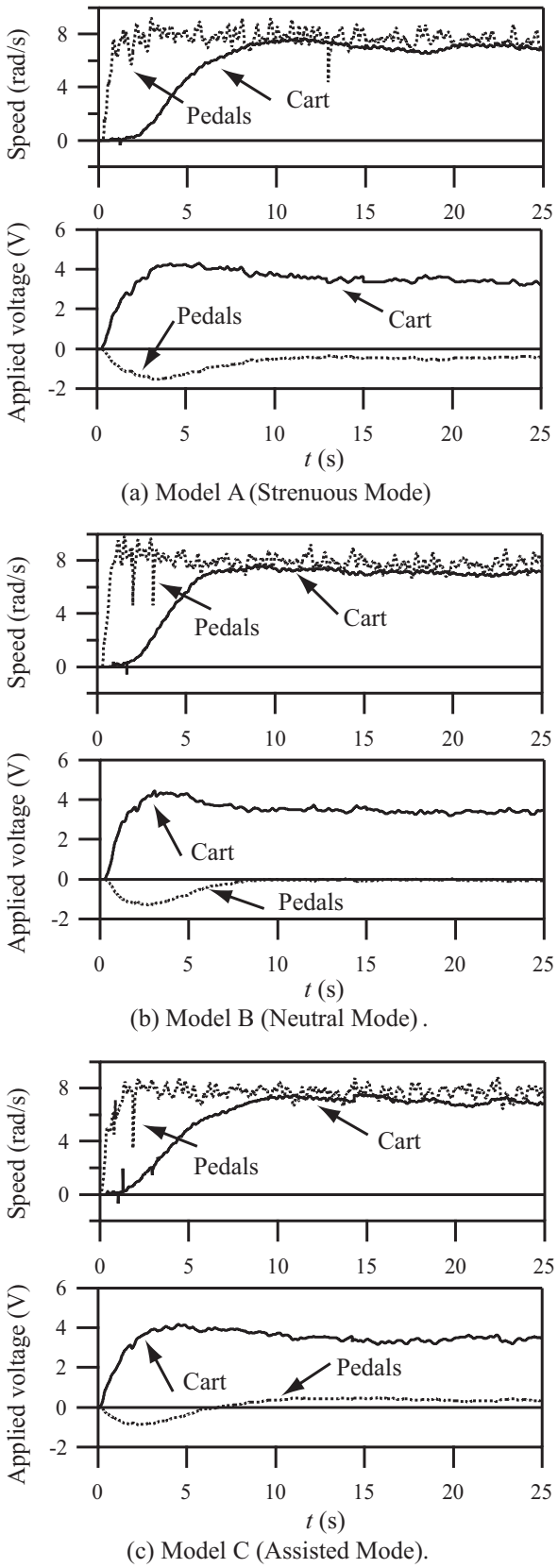

Fig. 8. Experimental results for flat road.

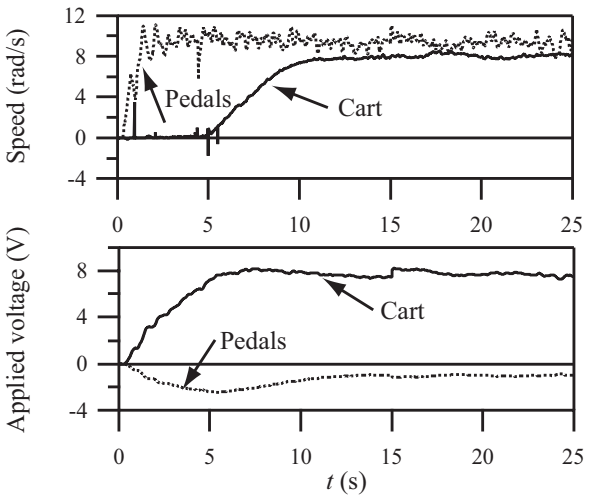

(a) Model A (Strenuous Mode).

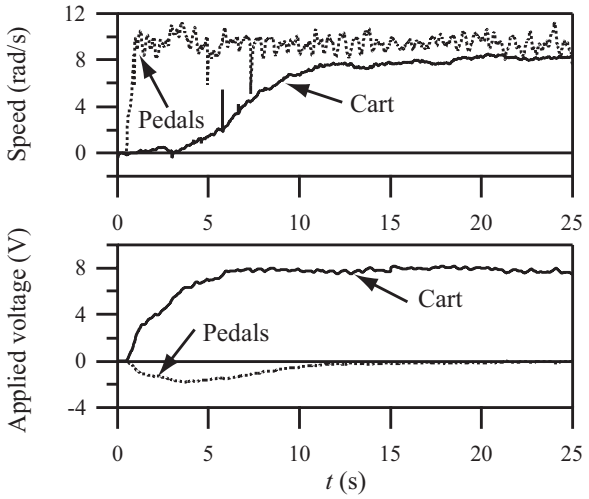

(b) Model B (Neutral Mode).

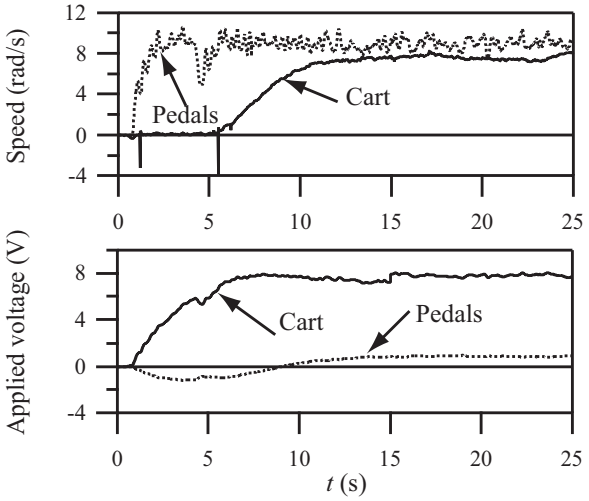

(c) Model C (Assisted Mode).

Fig. 9. Experimental results for uphill slope.

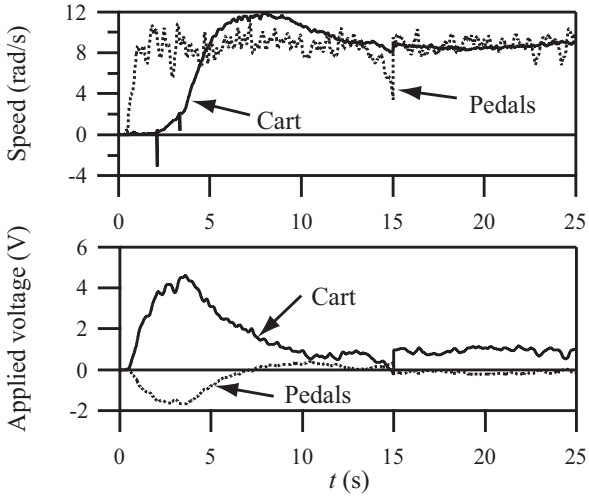

(a) Model A (Strenuous Mode).

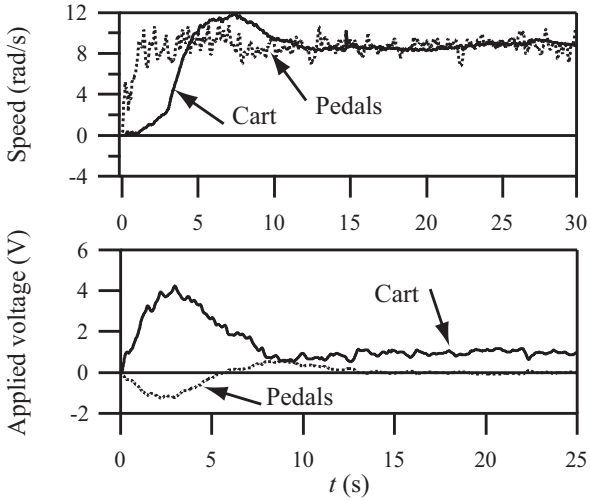

(b) Model B (Neutral Mode).

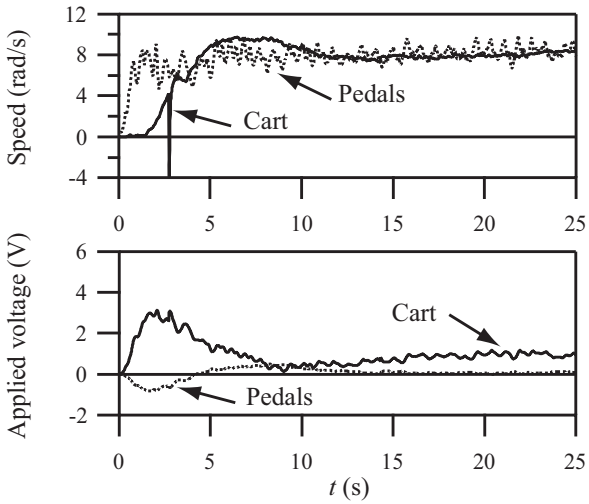

(c) Model C (Assisted Mode).

Fig. 10. Experimental results for downhill slope.